Synthesis of large monolayer single crystal MoS_2 nanosheets with uniform size through a double-tube technology

Zhiyun Tu, Gaoda Li, Xia Ni, Leixin Meng, Suo Bai, Xiaobo Chen, Junjie Lou, and Yong Qin

Citation: Appl. Phys. Lett. **109**, 223101 (2016); doi: 10.1063/1.4968582
View online: http://dx.doi.org/10.1063/1.4968582
View Table of Contents: http://aip.scitation.org/toc/apl/109/22
Published by the American Institute of Physics

Synthesis of large monolayer single crystal MoS_2 nanosheets with uniform size through a double-tube technology

Zhiyun Tu,[1] Gaoda Li,[1] Xia Ni,[1] Leixin Meng,[1] Suo Bai,[1] Xiaobo Chen,[1] Junjie Lou,[1] and Yong Qin[1,2,a)]

[1]*Institute of Nanoscience and Nanotechnology, School of Physical Science and Technology, Lanzhou University, Lanzhou 730000, China*

[2]*The Research Institute of Biomedical Nanotechnology, School of Basic Medical Sciences, Lanzhou University, Lanzhou 730000, China*

(Received 28 August 2016; accepted 11 November 2016; published online 28 November 2016)

Two-dimensional MoS_2 attracts much attention because of its potential application in electronic and optoelectronic devices at present. However, the preparation of large and uniform single crystal MoS_2 nanosheets is still a challenge, which restricts its further application. Herein, monolayer single crystal MoS_2 nanosheets with large and uniform grain size have been synthesized by chemical vapor deposition using a double-tube system. Within the main growth area, the grain size reaches 146 μm on the substrate of SiO_2/Si, and the portion of MoS_2 nanosheets with grain size between 50 μm and 100 μm is up to 78%. Meanwhile, the grain size keeps constant in the direction perpendicular to the tubes and changes slightly in the parallel direction. This is attributed to the concentration distribution of intermediate product MoO_{3-x} in the one-side sealed inner tube set in a quartz tube, i.e., the double-tube system, which provides a way to the controllable and uniform synthesis of large monolayer single crystal MoS_2 nanosheets. *Published by AIP Publishing.*
[http://dx.doi.org/10.1063/1.4968582]

Two-dimensional (2D) transition metal dichalcogenides (TMDs) materials have attracted considerable attentions because of their potential in electronic and optical applications.[1,2] As a typical TMD with a direct bandgap of 1.8 eV, monolayer MoS_2 has been studied extensively in the past decade and is widely used in Field Effect Transistor (FET),[3] photocatalysis,[4] nanogenerator,[5] and sensors.[6] Since the electrical and optical properties of MoS_2 are influenced by the number of layers and grain boundaries,[7] great efforts have been exerted to synthesize monolayer MoS_2 with different methods, such as mechanical exfoliation,[1] liquid-phase exfoliation,[8] and chemical vapor deposition (CVD).[6,9–11] Among these methods, CVD is regarded as a potential method to synthesize monolayer MoS_2 with a large grain size in low cost and in a large scale.[12] During the preparation, the concentration of intermediate product MoO_{3-x} is crucial to the formation of MoS_2 and is affected by many parameters.[13] Previous studies have been focused on the effect of temperature,[14] ambient pressure,[7] gas flow,[15] and source materials.[16] However, the influence of the concentration of the intermediate product MoO_{3-x} on the growth of monolayer MoS_2 adjusted by the equipment structure has not been studied. In this work, monolayer MoS_2 nanosheets with a large and uniform grain size have been prepared in a large scale through a double-tube technology. The influences of source concentration on the concentration of MoO_{3-x} and the growth of monolayer MoS_2 have also been studied in theory.

MoS_2 grains were synthesized via the reaction of solid MoO_3 and S precursors. The reaction is governed by the equations[6,7,11,13]

$$MoO_3 + x/2\,S \rightarrow MoO_{3-x} + x/2\,SO_2, \quad (1)$$

$$MoO_{3-x} + (7-x)/2\,S \rightarrow MoS_2 + (3-x)/2\,SO_2. \quad (2)$$

The reaction proceeded at 850 °C in a double-tube system, which is composed of a one-side sealed inner tube and an outer quartz tube, as illustrated in Fig. 1(a). Compared with the previous work, the substrate was placed at the windward of MoO_3 source rather than leeward or top of MoO_3. Fig. 1(b) is an optical image of MoS_2 grains grown on a SiO_2 (300 nm)/Si substrate. The grain size of MoS_2 is 146 μm. It is the largest grain size of monolayer MoS_2 grown on the SiO_2/Si substrate so far. The monolayer MoS_2 with a large grain size was directly synthesized on the substrate, and further fabrication of devices can be done on this readily available SiO_2/Si substrate without any transference of MoS_2 grain. The atomic force microscope (AFM) image in Fig. 1(c) shows that the surface of MoS_2 grain is smooth and the AFM height profile in the inset reveals that the thickness of the MoS_2 nanosheet is about 0.8 nm, which corresponds with the thickness of monolayer MoS_2 based on the previous report.[17] To confirm the layer number of the grain, Raman characterization is also carried out using a 532 nm laser at room temperature. The result shown in Fig. 1(d) exhibits two characteristic bands at 383.1 cm^{-1} with the full-width-half-maximum (FWHM) values of 6.0 cm^{-1} and 402.3 cm^{-1} with the FWHM values of 4.2 cm^{-1}, which correspond with Raman active modes of in-plane ($E_{2g}{}^{-1}$) and out-of-plane (A_{2g}) vibrations, respectively. The difference in frequency between the two vibration modes is 19.2 cm^{-1}, which correlates with the results of monolayer MoS_2 grains.[11] Meanwhile, the optical property of MoS_2 grains is characterized by photoluminescence (PL) spectrum at room temperature (Fig. S1(a)). A strong PL scatter is observed, and the intensity peak at 1.84 eV is in accordance with the band energy of monolayer MoS_2. Both the results confirm that the MoS_2 grains are monolayer.

a)E-mail: qinyong@lzu.edu.cn

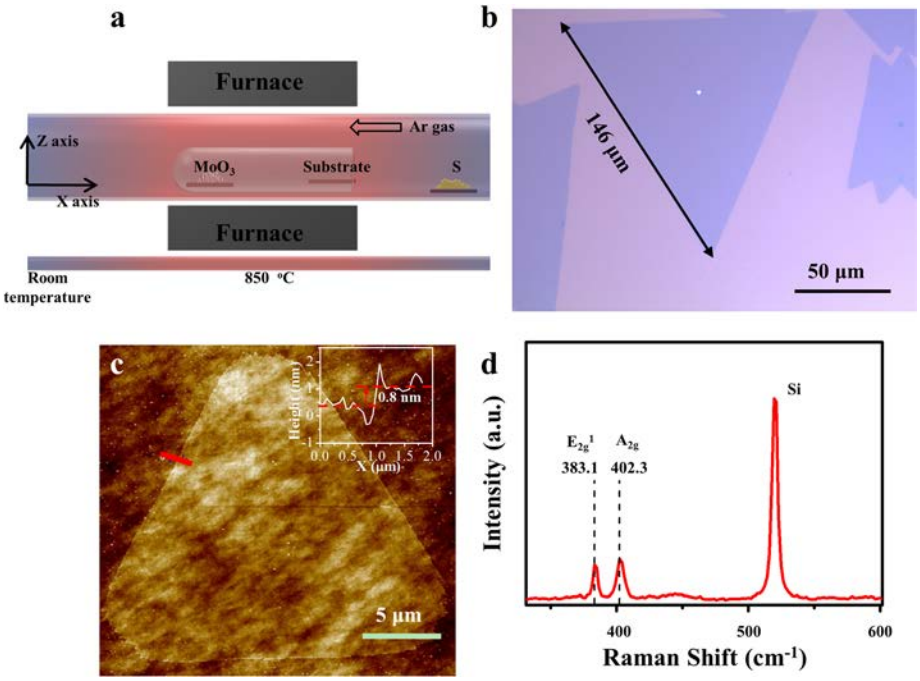

FIG. 1. Growth of large-grain MoS_2: (a) The schematic illustration of the experimental set-up. The coordinate is a right-hand coordinate system. (b) The optical image of the obtained triangular MoS_2 grains. (c) The AFM image of monolayer MoS_2 on the SiO_2/Si substrate. (The inset is an AFM cross-sectional profile along the line indicated in (c), which shows the thickness of MoS_2 is 0.8 nm.) (d) Raman spectrum of the MoS_2 grain on the SiO_2/Si substrate.

Fig. 2(a) is an optical image of a sample. The area covered by MoS_2 is divided into nine parts and numbered in sequence. Fig. 2(b) is scanning electron microscopy (SEM) images of MoS_2 grain in Areas 1–9. The result shows that the MoS_2 grains grow densely. The size of the grains has a distribution between 40 and 100 μm and displays an excellent uniformity along the Y-axis direction. Meanwhile, the layer number of a random spot locating on MoS_2 nanosheets

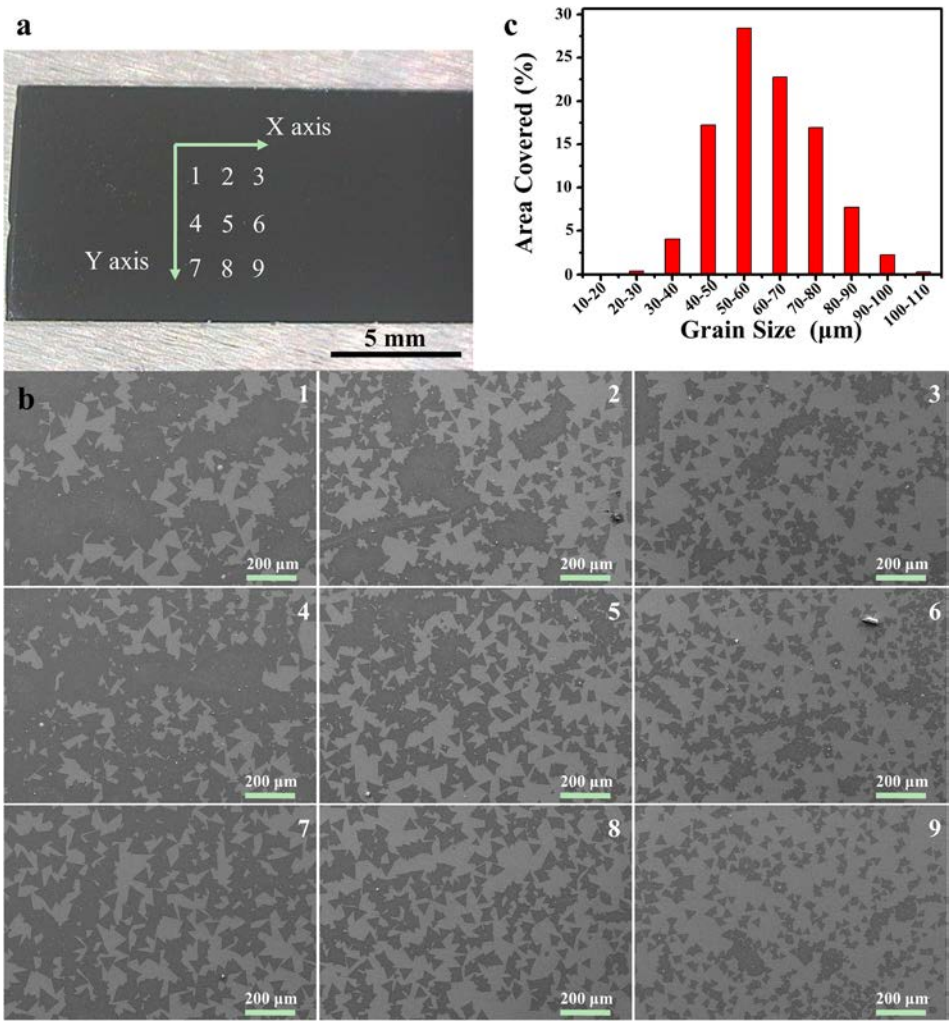

FIG. 2. (a) The optical image of MoS_2 on the SiO_2/Si substrate. The area is divided into nine parts. (b) SEM images of MoS_2 grain in Areas 1–9. (c) The size distribution of monolayer MoS_2 grains.

in each of the nine areas is characterized by Raman spectrum and shown in Fig. S1(b). The difference between two typical peaks corresponds with that of monolayer MoS_2 in all nine spectra. Fig. 2(c) shows the statistical distribution of the grain size of monolayer MoS_2 nanosheets in Fig. 2(b) according to the previous reported approach.[18] Statistical result shows that the MoS_2 grains with the grain size between 50 μm and 100 μm occupy 78% of the total area of the MoS_2 grains, a higher degree of uniformity of the grain size compared with previous works synthesized on the SiO_2/Si substrate.[17,18]

In order to clarify the relationship between the concentration of the intermediate product MoO_{3-x} and the formation of monolayer MoS_2, distributions of MoS_2 nanosheet's grain size along the X and Y axes are counted and shown in Figs. 3(a) and 3(b), respectively. An increase of grain size along the negative X axis and a uniform grain size along the Y axis are observed. The variations of grain size are supposed to be related to the concentration distribution of the intermediate product MoO_{3-x}, which results from the concentration distributions of MoS_2 and S source along the corresponding directions.

To further study the concentration distribution in tube and its influence on the growth of monolayer MoS_2 nanosheets, the finite element method is used to simulate the concentration distributions of MoS_2 and S sources according to diffusion equations (Fig. 3(c)). MoO_3 source is located at the left side (sealed side) of the inner tube, while S is located at the right side of the outer tube. Details of the simulation are explained in the supplementary material. It is widely supposed that an appropriate increase of concentration of MoO_{3-x} would lead to the increase of grain size of MoS_2.[11,19]

In our work, the concentration of MoO_{3-x} is controlled by a one-side sealed inner tube. This inner tube can increase the concentration of sources by inhibiting their outward diffusion, which results in the gradient distribution of intermediate's concentration. Hence, the nucleation and growth of MoS_2 can be controlled easily. According to the numerical simulation, on the one hand, the concentration of MoO_3 and S is uniform along Y axis, which leads to the uniformity of grain size along this direction. On the other hand, the concentration of S remains almost constant while that of MoO_3 increases along the negative X axis, which leads to the increase of grain size along this direction. To further clarify the advantage of this double-tube system, the concentration distributions in the conventional setups (an inner tube with both sides opened or only outer tube) are compared with that in the double-tube system, shown in Fig. S3. It is evident that the concentration of MoO_3 and S is larger and that of S is much more uniform in double-tube system than that in the conventional setups. However, when the concentration of MoO_{3-x} further increases and exceeds a threshold, the nucleation is promoted and polycrystalline MoS_2 films or rectangular particles rather than monolayer nanosheets with large grain size are generated, which are shown in Fig. S2.

In summary, we synthesized monolayer MoS_2 with uniform and large grains by the CVD method in a double-tube system. The grain size of single monolayer MoS_2 on SiO_2/Si reaches 146 μm, and the portion of MoS_2 grains with size between 50 μm and 100 μm is up to 78%. The experimental results and a numerical simulation show that by the double-tube system, the concentration of intermediate product MoO_{3-x} can be controlled easily, which is of great importance to the growth of monolayer MoS_2 with large and uniform grain size.

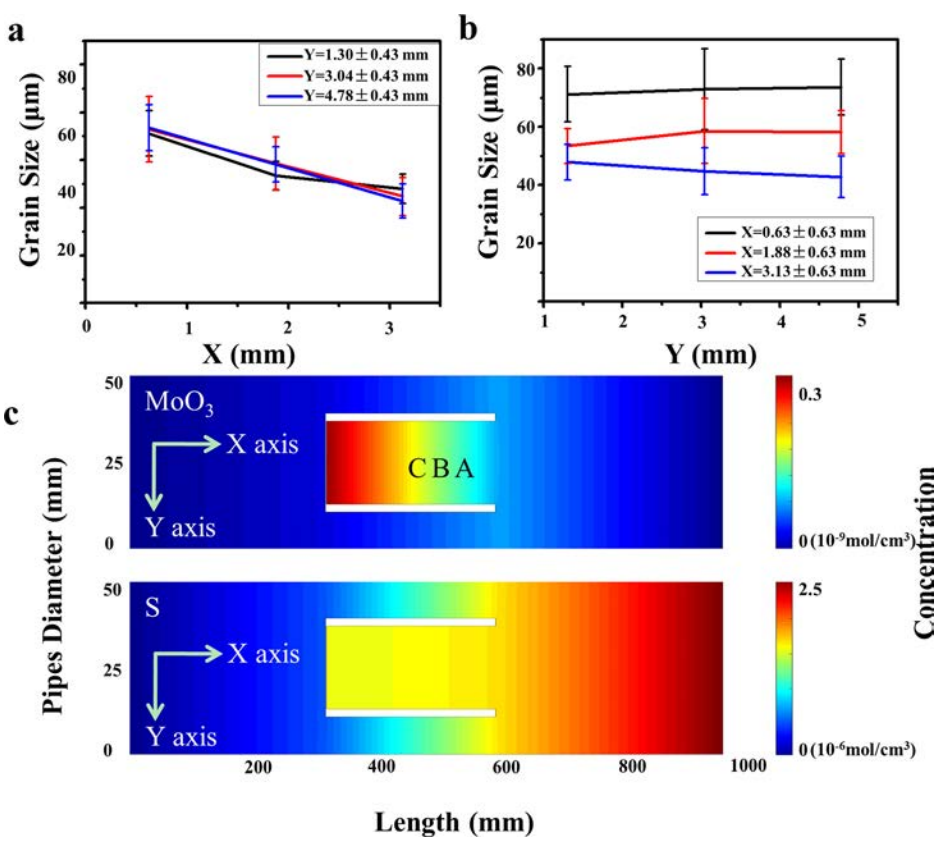

FIG. 3. The influence of source concentration on MoS_2 grain size: (a) Distributions of grain sizes along the X axis and (b) along the Y axis. (c) Numerical simulation of the source concentration distribution in tubes. Origin in (a) and (b) is based on the coordinate in Fig. 2(a).

See supplementary material for synthesis method and numerical simulation.

We sincerely appreciate the support from NSFC (Nos. 51322203, 51472111, 51302120), the National Program for the support of Top-notch Young Professionals, and the Fundamental Research Funds for the Central Universities (No. lzujbky-2016-k02).

[1]Q. H. Wang, K. Kalantar-Zadeh, A. Kis, J. N. Coleman, and M. S. Strano, Nat. Nanotechnol. **7**, 699 (2012).
[2]Q. Ji, Y. Zhang, Y. Zhang, and Z. Liu, Chem. Soc. Rev. **44**, 2587 (2015); M. Chhowalla, H. S. Shin, G. Eda, L. J. Li, K. P. Loh, and H. Zhang, Nat. Chem. **5**, 263 (2013).
[3]X. Zou, J. Wang, C. H. Chiu, Y. Wu, X. Xiao, C. Jiang, W. W. Wu, L. Mai, T. Chen, J. Li, J. C. Ho, and L. Liao, Adv. Mater. **26**, 6255 (2014); R. Kappera, D. Voiry, S. E. Yalcin, W. Jen, M. Acerce, S. Torrel, B. Branch, S. Lei, W. Chen, S. Najmaei, J. Lou, P. M. Ajayan, G. Gupta, A. D. Mohite, and M. Chhowalla, APL Mater. **2**, 092516 (2014).
[4]W. Zhou, Z. Yin, Y. Du, X. Huang, Z. Zeng, Z. Fan, H. Liu, J. Wang, and H. Zhang, Small **9**, 140 (2013).
[5]J. Feng, M. Graf, K. Liu, D. Ovchinnikov, D. Dumcenco, M. Heiranian, V. Nandigana, N. R. Aluru, A. Kis, and A. Radenovic, Nature **536**, 197 (2016); W. Wu, L. Wang, Y. Li, F. Zhang, L. Lin, S. Niu, D. Chenet, X. Zhang, Y. Hao, T. F. Heinz, J. Hone, and Z. L. Wang, *ibid.* **514**, 470 (2014).
[6]J. Xia, X. Huang, L. Z. Liu, M. Wang, L. Wang, B. Huang, D. D. Zhu, J. J. Li, C. Z. Gu, and X. M. Meng, Nanoscale **6**, 8949 (2014).
[7]S. Najmaei, Z. Liu, W. Zhou, X. Zou, G. Shi, S. Lei, B. I. Yakobson, J. C. Idrobo, P. M. Ajayan, and J. Lou, Nat. Mater. **12**, 754 (2013).
[8]Z. Zeng, Z. Yin, X. Huang, H. Li, Q. He, G. Lu, F. Boey, and H. Zhang, Angew. Chem. - Int. Ed. **50**, 11093 (2011); M. A. Hussain, M. Yang, T. J. Lee, J. W. Kim, and B. G. Choi, J. Colloid Interface Sci. **451**, 216 (2015).
[9]K. Kang, S. Xie, L. Huang, Y. Han, P. Y. Huang, K. F. Mak, C. J. Kim, D. Muller, and J. Park, Nature **520**, 656 (2015).
[10]K. K. Liu, W. Zhang, Y. H. Lee, Y. C. Lin, M. T. Chang, C. Y. Su, C. S. Chang, H. Li, Y. Shi, H. Zhang, C. S. Lai, and L. J. Li, Nano Lett. **12**, 1538 (2012); H. Schmidt, S. Wang, L. Chu, M. Toh, R. Kumar, W. Zhao, A. H. Neto, J. Martin, S. Adam, B. Ozyilmaz, and G. Eda, *ibid.* **14**, 1909 (2014); Y. C. Lin, W. Zhang, J. K. Huang, K. K. Liu, Y. H. Lee, C. T. Liang, C. W. Chu, and L. J. Li, Nanoscale **4**, 6637 (2012).
[11]Y. H. Lee, X. Q. Zhang, W. Zhang, M. T. Chang, C. T. Lin, K. D. Chang, Y. C. Yu, J. T. Wang, C. S. Chang, L. J. Li, and T. W. Lin, Adv. Mater. **24**, 2320 (2012).
[12]W. Chen, J. Zhao, J. Zhang, L. Gu, Z. Yang, X. Li, H. Yu, X. Zhu, R. Yang, D. Shi, X. Lin, J. Guo, X. Bai, and G. Zhang, J. Am. Chem. Soc. **137**, 15632 (2015).
[13]X. L. Li and Y. D. Li, Chem. Eur. J. **9**, 2726 (2003).
[14]J. Shi, X. Zhang, D. Ma, J. Zhu, Y. Zhang, Z. Guo, Y. Yao, Q. Ji, X. Song, Y. Zhang, C. Li, Z. Liu, W. Zhu, and Y. Zhang, ACS Nano **9**, 4017 (2015).
[15]Y. Cao, X. Luo, S. Han, C. Yuan, Y. Yang, Q. Li, T. Yu, and S. Ye, Chem. Phys. Lett. **631–632**, 30 (2015).
[16]S. Wang, Y. Rong, Y. Fan, M. Pacios, H. Bhaskaran, K. He, and J. H. Warner, Chem. Mater. **26**, 6371 (2014).
[17]S. Wu, C. Huang, G. Aivazian, J. S. Ross, D. H. Cobden, and X. Xu, ACS Nano **7**, 2768 (2013).
[18]A. M. van der Zande, P. Y. Huang, D. A. Chenet, T. C. Berkelbach, Y. You, G. H. Lee, T. F. Heinz, D. R. Reichman, D. A. Muller, and J. C. Hone, Nat. Mater. **12**, 554 (2013).
[19]Q. Fu, W. Wang, L. Yang, J. Huang, J. Zhang, and B. Xiang, RSC Adv. **5**, 15795 (2015).